

Monte Carlo Simulation of Ethylene Hydrogenation on Pt Catalysts

Dario Duca,^{*,1} László Botár,[†] and Tamás Vidóczy^{†,2}

^{*} *Istituto di Chimica e Tecnologia dei Prodotti Naturali del CNR, Via Archirafi 26, 90123 Palermo, Italy;* [†] *Central Research Institute for Chemistry of the Hungarian Academy of Sciences, Pusztaszeri út 59-67, H-1025 Budapest, Hungary*

Received October 23, 1995; revised March 29, 1996; accepted April 30, 1996

The catalytic hydrogenation of ethylene on Pt catalysts was simulated by a Monte Carlo model. Elementary events such as adsorption, diffusion, and desorption of the species involved (hydrogen, ethylene, and ethane) and reaction on the surface were considered. Based on comparison between experimental and calculated data no distinction has to be made between competitive and non-competitive hydrogen adsorption sites nor has adsorbed hydrogen activation to be taken into consideration. However, steric hindrance caused by adsorbed ethylene and ethane has been included in the model. Not only was the basic physical and chemical behavior reproduced by this very simple model, but also important experimental findings such as the trend of the turnover frequency versus hydrogen pressure (p_{H_2}) and the magnitudes of reaction orders for hydrogen and ethylene. In addition this model can predict some aspects of hydrocarbon hydrogenation not investigated experimentally so far.

© 1996 Academic Press, Inc.

1. INTRODUCTION

Hydrogenation of ethylene on Pt group catalysts, a process investigated extensively experimentally, is a good model for the study of the catalytic hydrogenation in general, since the Horiuti–Polanyi mechanism, consisting of a canonical Langmuir–Hinshelwood process involving two reactants and one reaction product is well accepted.

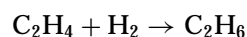
Recently, new experimental results have been presented (1–4) and employed for studying this reaction with a new approach, namely, micro-kinetic analysis (4). This approach uses deterministic methods (i.e., the solution of ordinary differential equation systems (ODES) (5) for the estimation of the kinetic parameters. However, it is almost impossible to rationalize surface phenomena such as diffusion, activation, and steric hindrance of the surface species with the ODES approach. Additionally, the deterministic methods require direct information about the surface species and sites at the microscopic level and assignment of the initial values of a surface molar ratio to the above species and sites (2) before starting the calculation.

The above difficulties are avoided in this study by using a stochastic model (6) which simulates the catalytic reaction better, owing to the possibilities of taking into account the characteristics of the surface species involved. The model is defined by:

- (a) the composition of the reactant mixture,
- (b) the metal catalyst surface (simulated by a squared matrix large enough (7, 8) in order to avoid size effects),
- (c) the formal definition of the morphology (8, 9) of the surface,
- (d) the possible events between the molecules in the gas-phase and the metal catalyst surface and those between the species occupying the surface sites,
- (e) the probabilities of occurrence of the events in d.

Conditions a–c are related to the experimental characteristics of the catalytic system, d is related to the elementary steps involved in the observable reaction, and e is related to the kinetics of the observable reaction through the kinetics of the elementary steps defined in d.

Here we report the results of a study of the reaction:



under pseudo steady-state conditions.

The choice of the ethylene hydrogenation is due to the formal simplicity of the chemical process, to the importance of olefin catalytic hydrogenation, and to the possibility of using the results as the basis for the study of more complicated hydrogenations.

2. THE MODEL

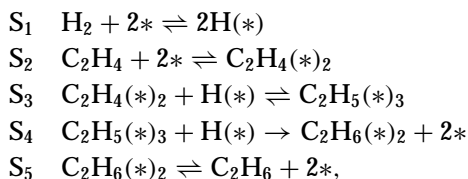
2a. General Aspects

Monte Carlo models have been suggested as a tool for studying simple catalytic or more generally surface reactions (10); moreover, these studies have recently been applied successfully in investigating practical aspects (11) of catalysis. However, to the best of our knowledge, Monte Carlo simulation of catalytic hydrogenation on a metallic surface has never been performed.

¹ E-mail: ictpn@cuc.unipa.it.

² E-mail: tvid@cric.chemres.hu.

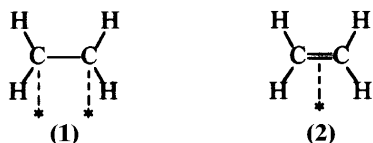
The following steps have been used as the basis for the reaction of ethylene hydrogenation,



where * and (*) represent empty and occupied catalyst sites respectively and $X(*)_n$ is a generic species X interacting with n catalyst sites. Although other steps such as adsorption of H_2 on competitive or non-competitive sites, diffusion of H on the surface from non-competitive to competitive sites and H activation on the surface have been considered earlier in the literature (1–4), they were not applied in this Monte Carlo model, the model performance being adequate without such steps (see below).

Steps S_1 , S_2 , and S_5 are the adsorption–desorption steps for hydrogen, ethylene, and ethane, respectively, and they represent six among the possible events involved in the reaction. Hydrogen is dissociated and adsorbed in atomic form (S_1) while ethylene and ethane are adsorbed on two catalytic sites (S_2 , S_5).

Three different forms (12) have been suggested in the literature for ethylene adsorption on a metallic surface, the σ , the π (1 and 2 below, respectively) and the ethylidinic forms.



In our simulation we can avoid making distinction among them because species 1 and 2, although interacting with a different number of surface sites have an analogous steric arrangement on the surface. Therefore, being the only elementary surface events considered, they have equivalent behavior in the surface reactivity simulation. Furthermore, the ethylidinic species may be considered in the experimental conditions (1–4) simulated in this study as surface poisoning (12, 13) formed during the reaction but, as they do not react and the experimental results are normalised to the activity of non-poisoned (fresh) catalysts (see below), they do not affect the simulation. Moreover, the backward step S_1 shows that, before desorption of hydrogen, H_2 molecules must be formed on the catalyst surface.

Steps S_3 and S_4 are the surface reaction steps. S_3 is considered only formally; C_2H_5 is not treated as an individual species. It can either diffuse apart (see below), or react with another hydrogen atom (S_4). This simplification corresponds to the fact that S_3 has an activation barrier. In our model the probability of forming a C_2H_5 complex is

not less than unity; however, both ethylene and hydrogen retain their individual mobility within the complex. S_4 is the only irreversible step in the mechanism considered. In other words, hydrogenation occurs only when the right surface constellation is achieved; i.e., there are two hydrogens available immediately next to the two carbon atoms of an ethylene molecule.

All the surface species are allowed to diffuse on the surface but C_2H_5 moves by destroying the original surface species and reproducing adsorbed H and C_2H_4 . For this reason the diffusion of C_2H_5 is determined by the ethylene and hydrogen diffusion. The above simplification is supported by the results reported by Bond *et al.* (14, 15), who showed a very high probability of ethyl to ethylene reversion (backward step S_3) in ethylene hydrogenation on Pt catalysts. Therefore, on the catalyst surface only three species can diffuse and only these events are included in our simulation.

A steric hindrance parameter has been introduced in our model affecting the possible number of organic molecules which are close to each other. The parameter can take all integer values between 1 and 4 and this number represents the allowed number of nearest neighbor carbon atoms to any carbon atom. Since in these simulations we have mimicked the catalytic surface by a (100) metallic face (see below), the number of nearest neighbor sites \oplus of a generic site \otimes is four (1, below). We may find from one, the other C atom present in the molecule, to four carbon atoms close to any carbon atom adsorbed on the surface (2, below). Then



the lowest value of the steric hindrance parameter does not allow any contact between hydrocarbons while setting the highest value for the steric hindrance parameter in the simulation; all the sites next to an adsorbed ethylene may interact with other carbon atoms of different hydrocarbon molecules. It may be noted that the above hindrance parameter for values different from 4 introduces the concept of competitive (accessible to hydrogen and ethylene) and non-competitive (accessible to hydrogen only) surface sites (4). Moreover, this Monte Carlo model easily identifies the activated hydrogen atoms (4) on the surface as the surface hydrogen atoms occupying sites that are the nearest neighbors of organic molecules.

The simulation of the metallic catalyst was performed by employing the (100) fcc Pt face mimicked by a 50×50 square matrix. It is important to emphasise the dependence of the results on the lattice size (7, 8, 16, 17). In the present case, however, it was verified that the results were not af-

ected by the size of the matrix when larger than 40×40 . The use of the (100) Pt face instead of a mixture of different metallic faces is correct since we limit the simulation to "structure insensitive" Pt catalysts (1, 18).

Experimental data of TOF versus p_{H_2} at a fixed temperature (4) were simulated using different probabilities corresponding to the different events. The applied values were well within their respective physically meaningful range.

2b. Details on the Simulations

The experimental TOF values of Pt catalyzed ethylene hydrogenation, simulated by our model, were obtained in a flow system. Results were not affected by diffusion phenomena (1, 4) and were normalized to fresh catalyst activity by employing experimental deactivation curves (TOF versus time) (1–4). Therefore, the typical problems of the catalytic ethylene hydrogenation, i.e., diffusion regime and deactivation of the catalysts (1, 4), are not considered in the present study.

The details of a Monte Carlo simulation applied to catalytic processes is known (e.g., (11)). Basically, probabilities are assigned to all possible events, like gas molecules striking the surface, adsorption and desorption, diffusion on the surface, reaction, taking place within a time-slice. Starting with an empty catalytic surface, a large number of time-slices are considered (typically 3×10^7), and the rate of reaction is calculated as the number of successful events (in this case the desorption of ethane) per real-time (see below) considered. Simulations were carried out until a quasi steady-state condition (constant rate of ethane formation) was obtained, and this rate was used to calculate TOF (reaction rate per catalytic site) values. The time units necessary for determining the real-time and then for calculating the reaction rate and TOF were determined on the basis of the equation derived from the kinetic gas theory considering the number of hits of hydrogen molecules per unit surface area per unit time (F_{H_2}) as a function of the pressure of hydrogen (p_{H_2}),

$$F_{\text{H}_2} = p_{\text{H}_2} / (2\pi m_{\text{H}_2} k_{\text{B}} T)^{1/2}, \quad [1]$$

where k_{B} refers to the Boltzmann constant, m_{H_2} refers to the molecular mass of hydrogen, and T refers to the temperature. Thus, knowing p_{H_2} and T , an internal timer can be defined using F_{H_2} and the probability of a hydrogen molecule hitting the surface in a time-slice.

Since experimental TOF values are normalised to the activity of the fresh catalysts we have not considered ageing or poisoning phenomena on the catalyst surface; the model however, is also suitable for the study of such phenomena. Moreover, as this study aims to demonstrate the potentiality of the Monte Carlo method in describing the kinetics of surface reactions, parameters reported in the literature were used where available.

The sticking probability of ethane on the surface (σ) was considered to be zero (19, 20) because the molecules of ethane produced in the reaction, once desorbed, are not readsorbed. This approximation, besides the much lower adsorption coefficient of ethane with respect to hydrogen and ethylene is also justified by the very low partial pressure of ethane in the reaction flow. Sticking probabilities of ethylene and hydrogen were considered as parameters in modelling the experimental TOF versus p_{H_2} values. Moreover, the values of σ in the literature are quite varied and in the present case the reported sticking probability on a clean surface for hydrogen and ethylene ranges between 10^{-1} – 10^{-3} and 10^{-1} – 10^{-2} , respectively (4).

The desorption probabilities (δ) were considered to be proportional to the surface coverage of the different species and in particular the proportionality coefficient was considered to be 1 for ethane. The above approximation is the equivalent of the respective assumption of the Langmuir–Hinshelwood mechanism, namely that ethane, formed on the surface, is immediately desorbed. The proportionality coefficients for the hydrogen and ethylene desorption probabilities were taken, as easily demonstrable, equal to $2k\Delta t$, where Δt is the time-slice determined by F_{H_2} and the hitting probability of H_2 and k is the desorption rate constants (1, 4) of hydrogen or ethylene, determined at steady-state conditions. Since in the original works (1–4) hydrogen is considered as desorbed from two different kind of sites (competitive and non-competitive ones) and therefore characterized by two different rate constants, we have chosen to use an averaged value ($5.0 \times 10^4 \text{ s}^{-1}$) which is certainly within physically realistic limits.

Diffusion probabilities (Δ) were considered proportional to the surface coverage of the given species. Since diffusion is energetically more facilitated than desorption (the ratio of the activation energies $E_{a\Delta}/E_{a\delta}$ for the same species is close to 0.05) and the coefficient of proportionality in the ethane desorption probability being 1 (the highest allowed value), the coefficient of proportionality in the ethane diffusion probability was also taken as 1. The probability coefficients for the ethylene and hydrogen diffusion were considered variable parameters.

Finally, the probability of reaction was always unity; i.e., as soon as the right constellation of reactants occurred on the surface, reaction took place immediately.

The highest probability value used for any event was never larger than 0.1, so that to keep the error caused by not considering two events taking place simultaneously, i.e., in the same time-slice, below 1%; the corresponding experimental errors are certainly larger than the error caused by this approximation.

The random number generator (5) had different starting seeds for every event. It was shown that different starting seeds produce a standard deviation in the calculated TOF values not larger than 3%. Thus uncertainties inherent to

the Monte Carlo technique do not introduce errors larger than those originated by the experimental practice.

Our Monte Carlo program has been written in standard FORTRAN 77, so it could run on many different platforms. For the characteristics of the random number generator (5) employed in the program, the results of the simulations are equal even if obtained by different computers. Although for the final simulations we have used an IBM 3093 200 JVF (Centro di Calcolo dell'Università di Palermo), the program was also tested on a PC IBM 486 DX 66 MHz and on an IBM RISC/6000 workstation.

The average run-time for a simulation (i.e., one point in Fig. 2, see below) on the PC was about 2 h; the same lasted 4 min on the IBM 3093.

3. RESULTS AND DISCUSSION

The experimental values of TOF employed as reference, the corresponding values of p_{H_2} and some other information on the reaction system obtained from the original papers (1, 4) are reported in Table 1. In Fig. 1, the simulated molar ratios for the surface species and empty sites are reported for one particular experimental condition. Considering that, for all the other experimental situations, simulations gave similar curves and that TOF values were determined from the final part of the simulation (TOF was typically calculated on the last 6.25×10^6 time-slices), it is evident that the activity of the catalyst is determined un-

TABLE 1

Summary of Experimental Data Used in the Comparison^e

Temperature (K)	Catalyst ^a	Ethylene pressure (kPa)
298.15	0.04% Pt/Cab-O-Sil	3.3
Hydrogen pressure (kPa)		TOF ^b (s ⁻¹)
7.6		1.8
10.7		2.6
13.3		3.0
20.5		4.3
33.0		6.2
46.5		8.3
88.4		14.9
Reaction order for ethylene ^c		Reaction order for hydrogen ^d
-0.20		1.19

^a Catalyst synthesis and the low content of the metal results in platinum dispersion close to 1; however, since the reaction is insensitive to the catalyst structure, analogous behavior is expected for Pt catalysts having different genesis and dispersion (1-4).

^b Determined from data reported in Ref. (4, p. 130, Fig. 5.3).

^c Evaluated at 298.15 K with hydrogen partial pressure 20.5 kPa and in the range of ethylene partial pressure of 0.67-10.7 kPa. At higher ethylene partial pressure the reaction order for ethylene tends to 0.

^d Evaluated from the data of the table. In the ethylene pressure range 0.66-10.0 kPa, the reaction order for hydrogen does not depend on the partial pressure of ethylene (1).

^e From Refs. (1-4).

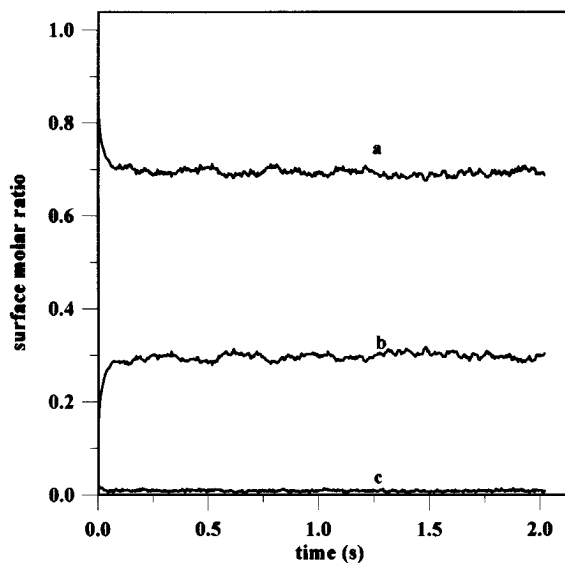


FIG. 1. Monte Carlo simulation for H_2 pressure 7.6 kPa. Plots of coverage θ for the differently occupied surface sites versus time: a. empty surface sites; b. C_2H_4 surface sites, and c. H surface sites. The curve of C_2H_6 (practically coincident with the time axis) is not reported for clarity.

der pseudo steady-state conditions. As pointed out in the preceding section, simulations have been performed employing constant and variable parameters. The latter were adjusted within a physically meaningful range of values in order to achieve a good fit between experimental and calculated TOF values. In this procedure a SIMPLEX program (5) was employed to change the values of the parameters and to stop the fitting procedure. It must be emphasized, however, that only a single TOF versus p_{H_2} curve (the one given in detail in Table 1) has been used in the fitting procedure; all other simulations were run using the optimal set of parameters.

The calculated TOF values are very close to the experimental ones and the experimental reaction orders of hydrogen and ethylene are fully reproduced by the simulation, thus validating the model.

Figure 2, plotted using logarithmic coordinates, shows the good agreement between the experimental and the simulated values of TOF versus p_{H_2} . The hydrogen reaction order determined employing the calculated points of TOF is 1.16 ($R^2 = 0.99$). Table 2 reports the parameters employed in the most satisfactory simulation. The sticking probabilities for both ethylene and hydrogen are close to the lowest, physically realistic limits. In general these low values of sticking probabilities are usually related to adsorption on polycrystalline Pt (4); however, in our case, experimental data were measured on very well dispersed Pt/silica (1-4) catalysts. Furthermore, the proportionality coefficients of desorption and diffusion probabilities are very similar to the corresponding ratio of the activation energy $E_{\text{a}\Delta}/E_{\text{a}\delta}$, generally close to 0.05.

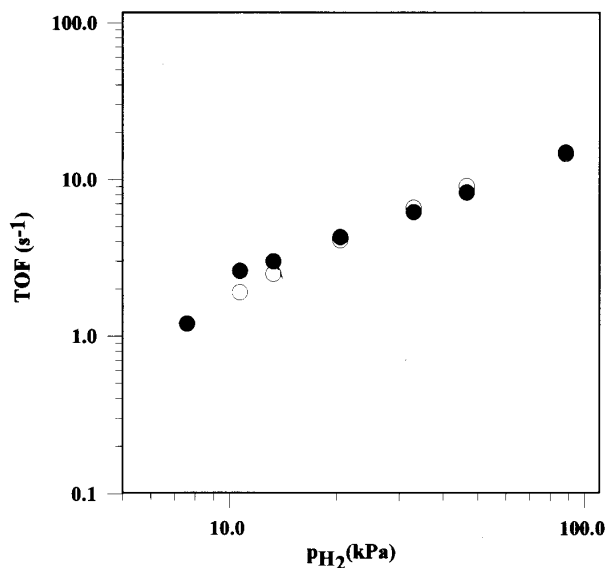


FIG. 2. Experimental (●) and calculated (○) TOF versus p_{H_2} (logarithmic scale).

The effects of the steric hindrance parameter on the simulation is shown in Fig. 3. It is evident that the shape of the curve TOF versus p_{H_2} strongly depends on this parameter and the simulated curve (TOF versus p_{H_2}) reproduces a realistic shape only when 1 is considered for the hydrocarbon steric hindrance parameter (corresponding to no contact allowed between adsorbed organic molecules). Interestingly, the same effect is noticed also when the other parameters have different values from those reported in Table 2. Thus this effect is, in our opinion, related to the demonstrated existence of different kinds of H sites (1–4, 21) on the catalyst surface. The hydrocarbon steric hindrance may be repre-

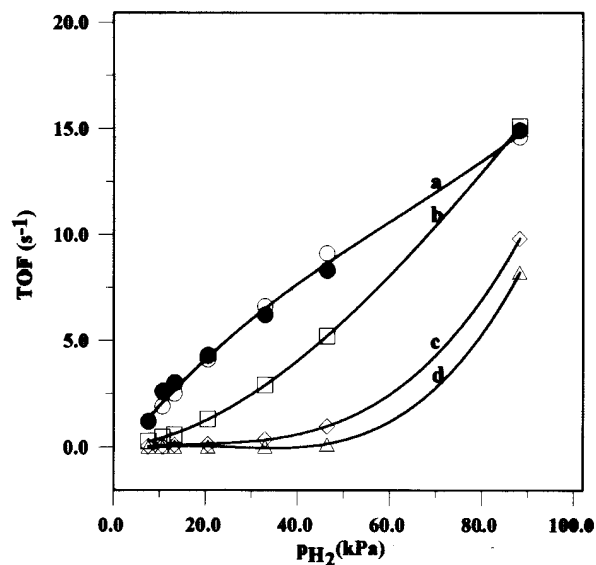


FIG. 3. Effect of steric hindrance parameter on TOF versus p_{H_2} curve. Experimental (●) and calculated points when steric hindrance parameter is equal to 1 (○), 2 (□), 3 (◇), and 4 (△). The curves are obtained by fitting cubic polynomials to experimental and simulated points.

sented in a more refined manner, and therefore, this important aspect will be further investigated.

Figure 4 shows the effect of the ethylene pressure on the calculated TOF at a partial hydrogen pressure of 20.5 kPa. The ethylene reaction order, at lower C_2H_4 partial pressure (the first four points) is -0.19 ($R^2 = 0.99$) while at higher values (the last three points) it is -0.06 ($R^2 = 0.98$). The last result is particularly important, as the experimental findings on the ethylene reaction order reported in Table 1 are completely reproduced, without using this set of experimental data for parameter estimation. In fact, the reaction order for hydrogen is directly calculated from the simulated TOF values obtained by the fitting procedure; thus a good agreement between theoretical and experimental TOF values forces the simulated hydrogen reaction order to be in accord with the experimental one. On the other hand, the values of TOF employed for determining the reaction order for ethylene are not used in the fitting procedure; therefore, the agreement between the calculated and experimental values contributes significantly to the validation of the model and of the parameter values reported in Table 2.

The fact that TOF decreases with increasing partial pressure of ethylene is interesting in its own right. The explanation of this unusual event (i.e., the decrease of TOF with the increase of the partial pressure of one of the reactants) can be readily obtained from studying the surface coverage of the various species. At ethylene pressures used in the calculations (greater than 2 kPa) the surface coverage of ethylene does not increase significantly (due to the steric hindrance there is not much room left for more ethylene molecules on the surface), so there is no gain in ethylene concentration

TABLE 2

Parameter Values Employed in the Final Simulation

σ_{H_2}	5.7×10^{-4}
$\sigma_{C_2H_4}$	4.3×10^{-2}
$\sigma_{C_2H_6}^a$	0.0
$\delta_{H_2}^a$	$1.0 \times 10^5 \cdot \theta_H \cdot \Delta t$
$\delta_{C_2H_4}^a$	$3.0 \theta_{C_2H_4} \cdot \Delta t$
$\delta_{C_2H_6}^a$	$1.0 \theta_{C_2H_6}$
Δ_{H_2}	$\delta_{H_2}/0.04$
$\Delta_{C_2H_4}$	$\delta_{C_2H_4}/0.08$
$\Delta_{C_2H_6}^a$	$\delta_{C_2H_6}/1.00$
Probability of reaction ^a	1
Steric hindrance parameter ^a	1

^a Fixed parameter.

Note. θ_X is the surface molar ratio of the generic species X. Note that θ_X is changing during the simulation. In the left-hand column, σ represents sticking to the surface, δ represents desorption, Δ represents diffusion. Δt is the time unit employed in evaluation of TOF. It depends on the H_2 pressure of the experiment and is determined by Eq. (1).

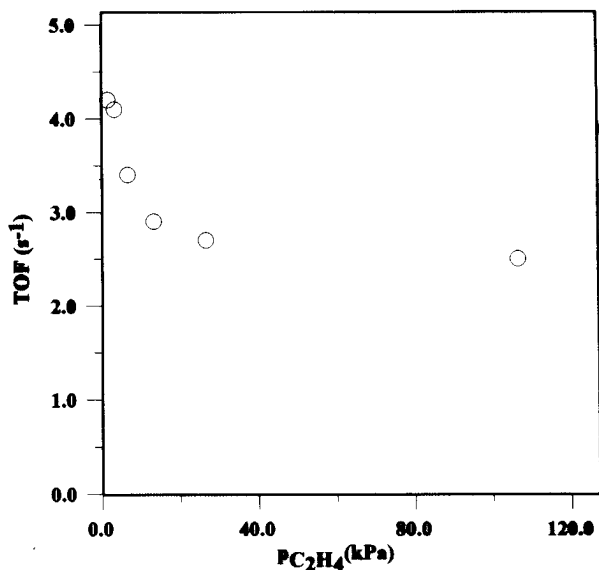


FIG. 4. Monte Carlo simulation TOF versus $p_{\text{C}_2\text{H}_4}$ trend ($p_{\text{H}_2} = 20.5$ kPa, $T = 298.15$ K).

on the surface. On the other hand, even a slight increase of ethylene coverage causes the catalytic sites available for hydrogen decrease significantly, thus the probability for the right surface constellation to result in a reaction decreases, i.e., with increasing ethylene partial pressure, TOF values decrease and approach a limiting value (due to the steric hindrance even in the case of total ethylene saturation there remain some sites for hydrogen). On the other hand, decreasing the partial pressure of ethylene should result in a clear maximum in TOF values, similar to the experimentally observed situation (23), which phenomenon was not fully understood at that time.

Another important aspect of the reaction captured by this model is shown in Fig. 5 where simulated TOF versus p_{H_2} values are reported at different ethylene pressures. The reaction order for hydrogen found experimentally (1) is not significantly influenced by ethylene pressure between 1.7 and 26.6 kPa, which feature was reproduced in the simulations correctly. The above results are related to a limitation of the hydrocarbon adsorption due to steric hindrance that strongly affects the amount of ethylene on the catalyst surface. This model predicts a range of ethylene partial pressure in which the reaction order for ethylene is positive. This range, which includes the lower limit of ethylene partial pressure 0, has not been investigated experimentally; thus the model can be used to study the reaction under conditions which are difficult, or even impossible, to obtain experimentally.

In order to investigate the properties of the model, some parameters were changed one by one, maintaining the values in a physically reasonable range (they were separately increased and decreased by a factor $10^{0.5}$).

Figure 6 shows the effect of these changes in the H_2 (a) and in the C_2H_4 (b) sticking probabilities. The reactivity decreased and increased with the decrease or increase of H_2 sticking probability. However, in the latter case, the slope of TOF versus p_{H_2} approaches zero at increasing values of p_{H_2} . As shown by the analysis of the surface coverage values, at low hydrogen pressure the ethylene is still much more abundant on the catalyst surface, so that increasing hydrogen on the surface does not significantly decrease surface coverage by ethylene; thus reactivity increases. The decrease of the slope in Fig. 6a for hydrogen pressures above 30 kPa is due to the fact that at high p_{H_2} the presence of ethylene on the surface diminishes drastically; so does the $\text{C}_2\text{H}_4/\text{H}_2$ surface ratio with the result that the H_2 adsorption-desorption equilibrium becomes competitive with the reaction and the hydrogen reaction order must decrease. This effect, due to increased hydrogen sticking probability, is equivalent to that observed experimentally on decreasing the reaction temperature (1) which also produces a lower value of $\text{C}_2\text{H}_4/\text{H}_2$ surface ratio.

The modifications in the values of TOF caused by the changes in C_2H_4 sticking probability are apparently more complex. On increasing the C_2H_4 sticking probability, TOF values lightly decrease in the range of hydrogen pressure 0–50 kPa while at higher hydrogen pressures TOF values increase. Conversely, on decreasing C_2H_4 sticking probability, at hydrogen pressures lower than 20 kPa, TOF values lightly increase, then decrease at higher hydrogen pressure. By analysis of the surface coverage, when the presence of ethylene on the surface is higher (higher ethylene stick-

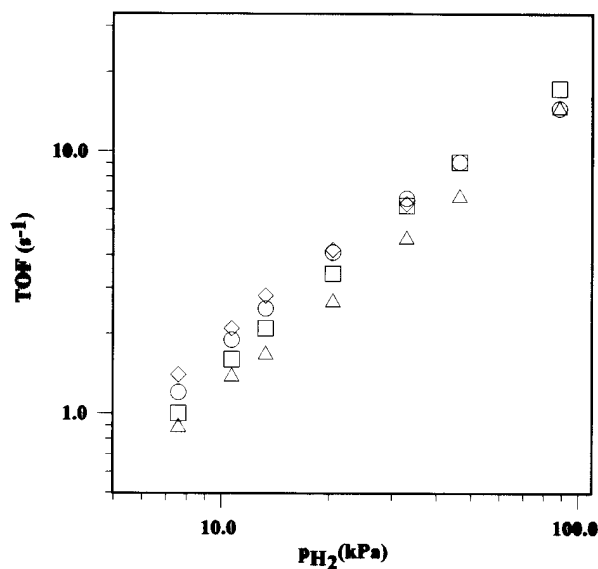


FIG. 5. TOF versus p_{H_2} (logarithmic scale) trends at different ethylene pressures. ($p_{\text{C}_2\text{H}_4} = 1.7$ kPa, \diamond ; = 3.3 kPa, \circ ; = 6.7 kPa, \square ; and = 26.6 kPa, \triangle). The slopes give the hydrogen reaction order (respectively 1.11 ($R^2 = 0.99$), 1.05 ($R^2 = 0.98$), 1.16 ($R^2 = 0.99$), and 1.12 ($R^2 = 1.00$)).

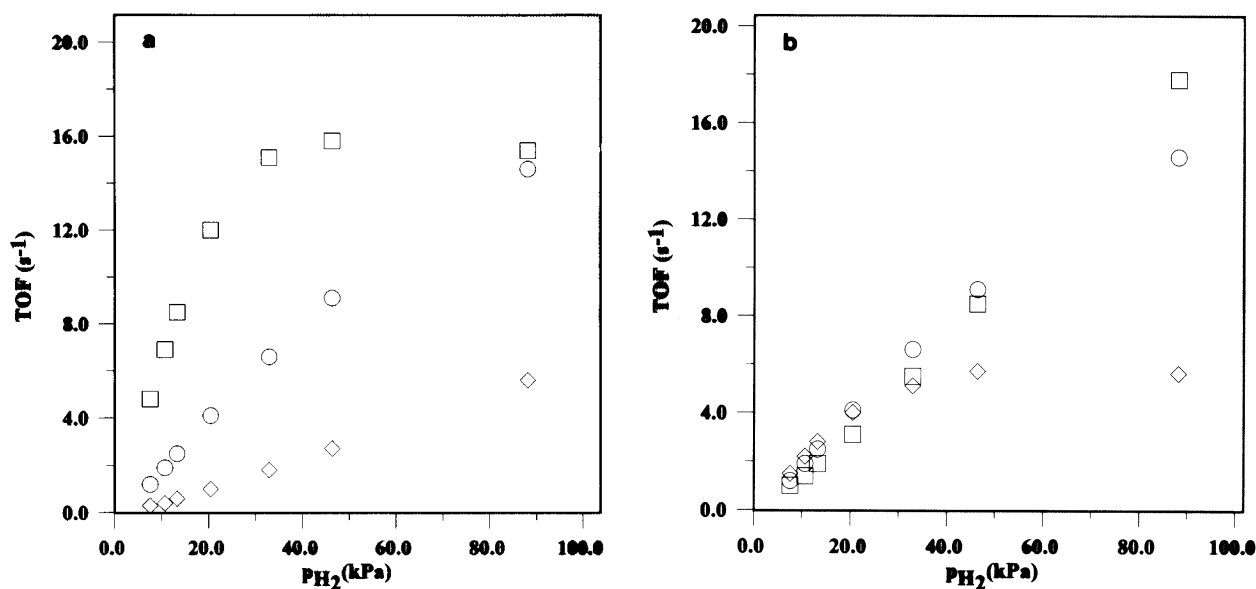


FIG. 6. Effect of changes in the sticking probability of hydrogen (a) and ethylene (b). TOF versus p_{H_2} , points obtained by parameter values as in Table 2, \circ ; points obtained increasing, \square ; and decreasing, \diamond ; the corresponding probability.

ing probability and/or lower hydrogen pressure) the abundance of surface hydrogen species determines the reactivity. At lower ethylene coverage (lower ethylene sticking probability and/or higher hydrogen pressure) when hydrogen surface coverage is very high, H_2 adsorption-desorption equilibrium becomes competitive with the reactivity, TOF decreases and the slope of TOF versus p_{H_2} becomes lower.

The effects on the reactivity caused by the equivalent changes of the desorption probabilities are opposite and less evident. Moreover, higher H or C_2H_4 diffusion probability increases reactivity but the effects due to H surface species were much more significant and at high H_2 pressures the effects on diminishing the hydrogen reaction order are observed.

The results show that this model reacts to changes in the simulation parameters and experimental conditions (p_{H_2} and $p_{C_2H_4}$) in agreement with experimental results and that in certain cases it is possible to anticipate probable trends in limiting situations under circumstances where experiments have not been performed.

Further experimental studies are needed both under steady-state (long time scale) and under "big-bang" (short time scale, transient) conditions, since such studies could give better values for the various parameters and information on the ageing and poisoning phenomena involved in the reaction.

Preliminary simulations on different catalytic systems indicate that this approach could have a general application in the studies of surface reactions. Further development of this model may be applied for the study of the industrial

processes like the hydrogenation of traces of acetylene in the presence of large amounts of ethylene and hydrogen on supported metal catalysts (22).

4. CONCLUSIONS

The stochastic model, based on a very simple set of events involving adsorption on the surface, desorptions from the surface, and moving on the surface, captures all the principal characteristics of the catalytic hydrogenation of ethylene. The resulting microscopic properties of the catalyst surface suggest a possible interpretation of the experimentally observed phenomena. The role and the influence of the different events involving the surface species are clear. Particularly interesting is the introduction of the steric hindrance parameter that is related to the existence of the competitive, non-competitive, and activated H sites. This model, although very simple, helps the understanding of some aspects of the ethylene hydrogenation reaction and enables prediction of the reactivity under experimental conditions which have not so far been investigated. It demonstrates that it is feasible to employ this very simple stochastic model to gather important information on microscopic events driving the macroscopic reaction with the help of easily accessible experimental results (e.g., TOF).

ACKNOWLEDGMENTS

We thank the bilateral agreement CNR-MTA and CNR (Progetto Finalizzato "Chimica Fine II" and Progetto Strategico "Tecnologia

Chimiche Innovative”) for financial support, the Calculation Centre of the Central Research Institute for Chemistry of the Hungarian Academy of Sciences for having supplied computer time on the IBM-RISC, and Mr. Péter Baranyai, Dr. Zsolt Kuti, Professor Gianfranco La Manna, and Professor Giulio Deganello for their criticisms and suggestions. D.D. thanks CNR for a leave of absence at KKKI-MTA of Budapest on behalf of the bilateral agreement CNR-MTA.

REFERENCES

1. Cortright, D., Goddard, S. A., Rekoske, J. E., and Dumesic, J. A., *J. Catal.* **127**, 342 (1991).
2. Goddard, S. A., Cortright, R. D., and Dumesic, J. A., *J. Catal.* **137**, 186 (1992).
3. Rekoske, J. E., Cortright, R. D., Goddard, S. A., Sharma, S. B., and Dumesic, J. A., *J. Phys. Chem.* **96**, 1880 (1992).
4. Dumesic, J. A., Dale, F. R., Aparicio, L. M., Rekoske, J. E., Treviño, A. A. (Eds.), “The Microkinetics of Heterogeneous Catalysis,” p. 113, ACS Professional References book, Am. Chem. Soc. Washington, DC, 1993.
5. Press, W. H., Teukolsky, S. A., Vetterling, W. T., and Flannery, B. P., “Numerical Recipes,” Cambridge Univ. Press, Cambridge, 1992.
6. Ziff, R. M., Gulari, E., and Barshad, Y., *Phys. Rev. Lett.* **56**, 2553 (1987).
7. Sadiq, A., *Z. Phys. B Condensed Matter* **67**, 211 (1987).
8. Meakin, P., and Scalapino, D. J., *J. Chem. Phys.* **87**, 731 (1987).
9. Ehsasi, M., Matloch, M., Frank, O., Block, J. H., Christmann, K., Rys, F. S., and Hirschwald, W., *J. Chem. Phys.* **91**, 4949 (1989).
10. Kaya, H., Erzan, A., and Kadirgan, F., *J. Chem. Phys.* **98**, 9030 (1993).
11. Herz, R. K., Badlani, A., Schryer, D. R., and Upchurch, B. T., *J. Catal.* **141**, 219 (1993).
12. Mohsin, S. B., Trenary, M., and Robota, H. J., *J. Phys. Chem.* **92**, 5229 (1988).
13. Zaera, F., and Somorjai, G. A., *J. Am. Chem. Soc.* **106**, 2288 (1984).
14. Bond, G. C., Phillipson, J. J., Wells, P. B., and Winterbottom, J. M., *Trans. Faraday Soc.* **60**, 1847 (1964).
15. Bond, G. C., Phillipson, J. J., Wells, P. B., and Winterbottom, J. M., *Trans. Faraday Soc.* **62**, 443 (1966).
16. Lutsevich, L. V., Elokhin, V. I., Myshlyavtsev, A. V., Usov, A. G., and Yoblonskii, G. S., *J. Catal.* **132**, 302 (1991).
17. Casties, A., Mai, J., and von Niessen, W., *J. Chem. Phys.* **99**, 3082 (1993).
18. Schlatter, J. C., and Boudart, M., *J. Catal.* **24**, 482 (1982).
19. Dumesic, J. A., Dale, F. R., Aparicio, L. M., Rekoske, J. E., Treviño, A. A. (Eds.), “The Microkinetics of Heterogeneous Catalysis,” p. 29, ACS Professional References book, Am. Chem. Soc. Washington, DC, 1993.
20. Sato, S., and Miyahara, K., *J. Res. Inst. Catal. Hokkaido Univ.* **23**, 1 (1975).
21. Sato, S., and Miyahara, K., *J. Res. Inst. Catal. Hokkaido Univ.* **22**, 51, 172 (1974).
22. Weiss, A. H., Gambhir, B. S., La Pierre, R. B., and Bell, W. K., *Ind. Eng. Chem. Process R&D* **16**, 352 (1990).
23. Margitfalvi, J., and Guzzi, L., *J. Catal.* **72**, 185 (1981).